Atomic Level Simulation of Permittivity of Oxidized Ultra-thin Si Channels

Stanislav Markov*, YanHo Kwok, GuanHua Chen
Dept. of Chemistry
The University of Hong Kong
Hong Kong SAR, China
*figaro@hku.hk

Gabriele Penazzi, Bálint Aradi, Thomas Frauenheim
BCCMS, University of Bremen, Bremen, Germany
Alessandro Pecchia,
University of Rome, "Tor Vergata", Rome, Italy

***Abstract*— We use density-functional-based tight binding theory, coupled to a Poisson solver to investigate the dielectric response in oxidized ultra-thin Si films with thickness in the range of 0.8 to 10.0 nm. Building on our recent work on the electronic structure of such Si films using the same formalism, we demonstrate that the electronic contribution to the permittivity of Si and of SiO_2 is modeled with good accuracy. The simulations of oxidized Si films agree well with available experimental data and show appreciable degradation of permittivity by nearly 18% at 0.8nm. Notable is however that simulations with hydrogenated Si substantially overestimate the degradation of permittivity. Beyond clarifying the quantitative trend of permittivity versus Si thickness, which is very relevant e.g. for fully-depleted Si-on-insulator MOSFETs, the present work is a cornerstone towards delivering an atomistic modelling approach that is free of material- or device-related phenomenological parameters.**

Keywords—permittivity; dielectric constant; silicon-on-insulator; density functional tight binding; atomistic simulations

I. Introduction

Recently we demonstrated an approach to model an extremely-thin Si-on-insulator (SOI) MOSFET atomistically, including explicitly an essential part of the gate- and buried oxides, and obtained good agreement in the sub-threshold region of the transfer characteristics against experimental data [8]. This was accomplished by coupling a density-functional-based tight binding (DFTB) Hamiltonian self-consistently to a Poisson solver and the non-equilibrium Green's functions formalism for transport. In a more comprehensive work we showed that DFTB, when carefully parameterized at the level of chemical elements, provides accurate description of the electronic structure of bulk Si and SiO_2 and of their interface [3]. It is not evident however, if the approach reliably models the dielectric screening in the semiconductor or the insulator, but this is of critical importance for MOSFET modeling. So the first goal of the present study is to evaluate the capability of DFTB to model the permittivity of oxidized ultra-thin Si films.

Besides the methodological incentive described above, we note that the dependence of permittivity on Si film thickness is not accurately known on a quantitative level. It is well understood that the reduction of Si film to a few nm thickness leads to degradation of the dielectric constant. A number of density-functional theoretical (DFT) studies of hydrogen-passivated Si films show that the degradation is quite strong, as much as 30–40% reduction at around 1 nm [4–6]. Experimental data of oxidized Si films down to 3.3 nm thickness shows less dramatic effect, but the scatter of the results prevents us from extrapolating reliably to sub-nm Si thickness [7]. Although several comprehensive theoretical studies have elucidated on the key factors leading to permittivity degradation and have mapped with atomic resolution the profile of permittivity across the Si/SiO_2 interface [16], [4], [17], to the best of our knowledge, the dependence on Si thickness have not been studied *ab initio*. Therefore, the second goal of our study is to establish the permittivity dependence on the thickness of oxidized ultra-thin Si films.

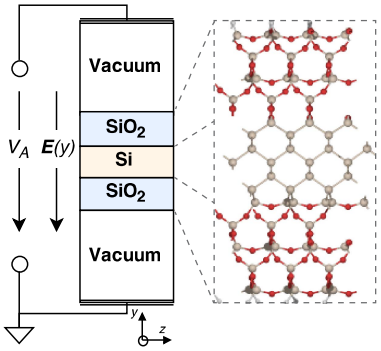

Fig. 1. Simulation setup and atomic model of the SiO_2-Si-SiO_2 structure (q-SiO_2 from [3]), periodic in x and z. Outer oxide planes are H-passivated, so that vacuum layer can be inserted. The applied bias V_A establishes electric field $E(y)$. We can find permittivity from continuity of electric displacement $\varepsilon_i E_i = \varepsilon_{i+1} E_{i+1}$, if we know a *macroscopic* field E_i across each layer.

II. Methodology

Our method for evaluating the dielectric constant is based on the continuity of electric displacement vector and follows previous studies [13][5]. The approach is best understood with the schematic diagram in Fig.1, which shows a five-layer system, including a three-layer atomic model of SiO_2-Si-SiO_2, with a vacuum layer outward of each SiO_2 layer. The system is quasi one-dimensional due to the imposed periodic boundary conditions in x and z. Assuming that each layer is linear and

This work was supported by University Grant Council of Hong Kong, within the Area of Excellence on Theory, Modeling and Simulation of Emerging Electronics under contract number AoE/P-04/08, and by the National Natural Science Foundation of China NSFC 21273186.

978-1-4673-7860-4/15/$31.00 ©2015 IEEE

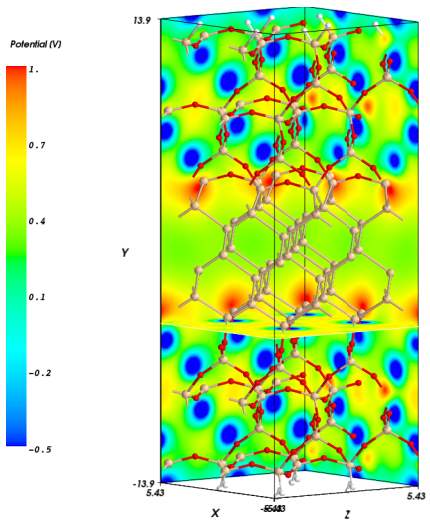

Fig. 2. Atomic model viewed off-<101> direction, and potential from the Poisson equation coupled to the DFTB Hamiltonian for three three different planes, orthogonal to the Cartesian axes; no applied bias. Note the large fluctuations around the atoms at the interface and in the oxide, which make it difficult to determine a macroscopic field E_i across each layer.

isotropic and lacking free carriers, e.g. as in a ground-state calculation at 0 K, the continuity of the displacement vector along y is expressed as $\varepsilon_i E_i(y) = \varepsilon_{i+1} E_{i+1}(y)$, where i and $i+1$ label two neighboring layers, ε_i and E_i being the permittivity and electric field. Given our knowledge of the vacuum permittivity ε_0, we can find the *macroscopic* permittivity of the SiO_2 and Si layers, if we determine the *macroscopic* field across each of them.

To accomplish the above we use the DFTB+ computer code [9], which implements the self-consistent-charge DFTB theory and optionally, a self-consistent coupling of the DFTB Hamiltonian to a Poisson solver [10–12]. DFTB derives from an approximation of density functional theory (DFT), and is much more efficient computationally at a comparable accuracy if carefully parameterized for Si and SiO_2 [3]. The enhanced efficiency arises from the fact that the two-center matrix elements of the Hamiltonian are pre-computed over extended neighbors, using non-orthogonal atomic basis, while three-center and crystal field terms are ignored. Parameterization of DFTB is done per chemical element and enables one to overcome the known issue of band-gap underestimation of DFT for common semiconductors and insulators. Beyond the tight-binding term in the Hamiltonian, DFTB includes an approximate term reflecting second-order charge density fluctuations that is computed self-consistently. This makes DFTB applicable to disordered materials and material interfaces, and we recently applied it successfully to study electronic structure in ultra-thin Si films passivated by amorphous and crystalline SiO_2 [3]. Here we extend the study to the dielectric response of such a system, noting that the term reflecting second-order density fluctuations captures not only permanent charge transfer, e.g. due to bond asymmetry, but also induced polarization due to applied electric field.

The atomic models used are those of SiO_2/Si super-cells with varying Si thickness and ~2 nm α-quartz SiO_2 used in

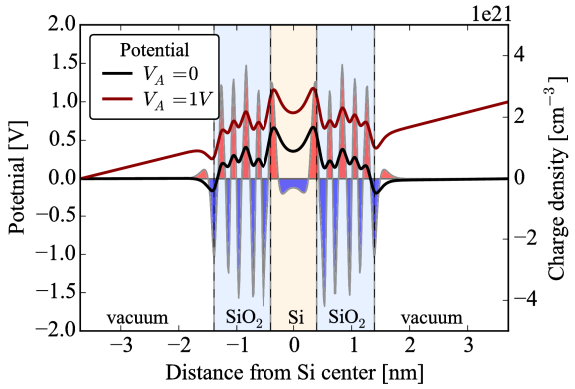

Fig. 3. Potential along the normal of the interface, averaged within *(xz)*-plane, for zero $\phi_0(y)$ and one volt $\phi_1(y)$ applied bias V_A (lines), and charge fluctuation density $\delta\rho_0(y)$ at $V_A = 0$ (filled curves) obtained from DFTB. Si layer is 0.8 nm thick in this case. Despite averaging in (*xz*), rapid fluctuations persist at atomic planes.

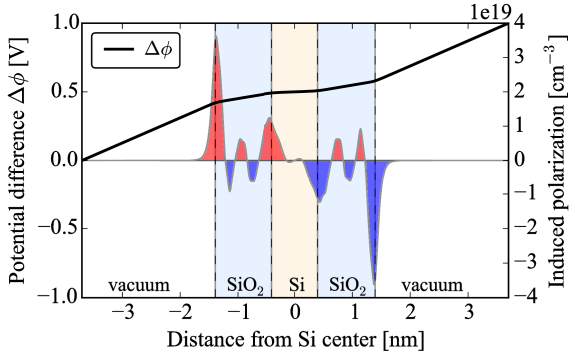

Fig. 4. Difference between the potential profiles from Fig. 3: $\Delta\phi = \phi_1 - \phi_0$, termed delta-potential (line), and difference between the fluctuation density from DFTB: $\rho_{ind} = \delta\rho_1 - \delta\rho_0$, i.e. induced polarization (filled curves). Subscripts label the applied biases. Notably, the delta-potential exhibits the character of a macroscopic electrostatic potential, linearly dropping with a rate dependent on the permittivity of the layer.

[14][3]. However, the oxide here is split in two and vacuum layer is inserted, hydrogen-passivating the outer surfaces of the oxide. A corresponding set of hydrogen-passivated Si films with 1.5 Å Si-H bond-length is also simulated for comparison, atomic structures are also from [3]; In the case of hydrogen passivation the conceptual model of Fig. 1 reduces to three layers only. All calculations in this work are performed at 0 K, with 8x1x8 point Monkhorst-Pack sampling of the Brillouin zone.

III. Results and Discussion

Coupling DFTB Hamiltonian to a Poisson solver allows us to find the distribution of the potential (ϕ) and electric field (E) in the model atomic structure under applied bias (V_A). The potential fluctuates rapidly with large magnitude, as shown in Fig. 2. We average the fluctuations in the planes parallel to the interfaces, taking advantage of the quasi one-dimensional nature of the model, but the rapid variation along the interface-normal (y-direction) remain, as shown in Fig. 3, and prevents us from directly evaluating a *macroscopic* electric field across each layer. It is important to note however, that the potential

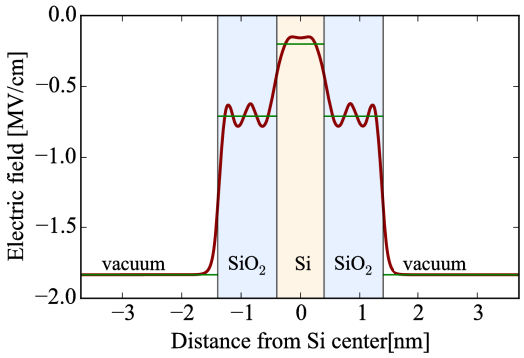

Fig. 5. Local electric field $E(y) = -\nabla\, \Delta\phi(y)$. The variations in the field are relatively small and averaging $E(y)$ yields the desired *macroscopic* field E_i for each layer, depicted as horizontal lines. From these, the dielectric constant of the 1 nm SiO_2 and 0.8 nm Si evaluate to 2.6 and 9.1, respectively. For a slightly thicker (1.3 nm) and thickest (8.3 nm) simulated Si films, we obtain 9.4 and 10.8, correspondingly.

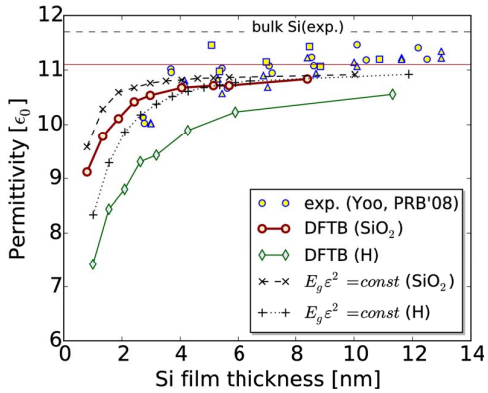

Fig. 6. Permittivity versus Si film thickness from our calculations (DFTB) is compared against a simple analytical model from Moss [15] and against experiment [7]. The value of $E_g(t_{Si})$ entering the model is the one predicted by DFTB [3]. The weaker dependence of the model (both for H and SiO_2 passivation of the channel) suggests that polarization at the interface plays critical role, and confinement itself cannot explain the total degradation of permittivity.

from DFTB arises from the net atomic charges only [12]. These are projected on the Poisson grid via exponentials with atom-specific rate, corresponding to the Hubbard value of the chemical element [10][12], where the Hubbard value is obtained *ab initio* from all-electron DFT calculation for each chemical element. The self-consistent charge fluctuation density is shown in Fig. 3 as shaded curve – red/blue shading for positive/negative charge. It has two components in principle – charge transfer, due to bond-asymmetry around the interface and in the oxide, and induced polarization, due to external electric field. The charge transfer component is by far dominant and in this work is common regardless of the applied bias V_A because we do not optimize the structure under bias. The induced polarization is present only under non-zero bias. Therefore, subtracting the charge-transfer component from the total fluctuations at non-zero bias yields the induced charge density, shown in Fig. 4 – note the scale of the right axis is 10 times smaller than in Fig. 3. If we also take the difference between the potential profiles of Fig. 3, i.e. with and without applied bias, we obtain the potential difference $\Delta\phi$, also shown in Fig. 4. This potential difference is readily interpreted as a macroscopic property, since it decays apparently linearly with different rate in each of the macro-layers of our system. From the negative gradient of $\Delta\phi$ we obtain the necessary *macroscopic* field, in order to evaluate the permittivity as outlined in the previous section. The resulting electric field $E(y)$ is shown in Fig. 5. It has small fluctuations around the layer-averaged *macroscopic* values, which are shown as solid horizontal lines. For the given film thickness of 0.8 nm Si and approximately 1 nm SiO_2 we find that the permittivity is 9.1 and 2.6 correspondingly. At the same time, our bulk dielectric constant for Si is evaluated at 11.1, which is approximately 5% lower than the known value of 11.7.

It is worthwhile noting that the magnitude of the electric field in Fig 5 is rather large, in comparison to previous studies [4], [6], [17]. Our purpose was to evaluate the dielectric response of the model under conditions relevant to transport simulations in a MOSFET, e.g. as in [8].

So far we showed the relevant quantities for the thinnest oxidized Si film of 0.8 nm. Besides, we have carried out the same procedure for both oxidized and hydrogenated Si films of different thickness up to 10.0 nm. The calculated permittivity as a function of Si film thickness is shown in Fig. 6. Compared with the available experimental data from [7], our simulation results of the oxidized Si films are in good agreement, while the hydrogenated Si films manifest substantially stronger degradation of permittivity with reducing film thickness. Our results for hydrogenated Si generally agree with previous DFT studies [4][6], despite the significant differences in the methodology and setup of the simulations.

The difference between hydrogenated and oxidized Si can already be anticipated from our study of the electronic structure of the corresponding films, where the band-gap enlargement with the reduction of Si thickness was overestimated by about a factor of two in the case of hydrogen passivation [3]. However, it has been established that the quantum confinement is not the principle reason for permittivity degradation [16][4][17]. To illustrate that this is the case in our work too, we make a comparison with a simple analytical model linking refraction index and band-gap to a constant, $E_g\varepsilon^2 = constant$, after [15]. Here E_g and ε are the band-gap and permittivity of Si at a given thickness; the constant is obtained from the corresponding bulk values, while $E_g(t)$ is from our previous study of the thickness-dependent band-gap [3]. The results from this model are also shown in Fig. 6, and we see that while it captures some of the decrease in permittivity, it nevertheless underestimates the total degradation.

In Fig. 7 we show the profile of the permittivity across the SiO_2/Si interface for several different thicknesses of Si. These profiles are obtained from the application of the continuity of the displacement vector on a *microscopic* level over $\Delta\phi$, for neighboring segments of the grid on which the Poisson equation is discretized along y. Given the fine grid of ~0.15 Å, we initially obtained some oscillations around the points of the interface and across the oxide. However applying Gaussian kernel filtering with a standard deviation of 1.15Å we obtained the relatively smooth profiles shown in Fig. 7. We note that

aaveraging the *inverse* permittivity in each material layer yields practically the same values as the ones obtained from the *macroscopic* field, reported in Fig. 6. Yet, having the local permittivity helps to understand the influence of the changes at the interface. We see in Fig. 7 that permittivity in the core Si varies weakly regardless of Si thickness. It determines the bulk permittivity in the limit of infinitely thick Si and evaluates to $11.1\varepsilon_0$, as stated earlier. The gradual transition of permittivity at the interface lowers the permittivity of Si and is a key reason for the overall degradation, as already shown in [4] and [17]. At the same time, it raises somewhat the permittivity of thin SiO_2, which in our case is $2.6\varepsilon_0$ – above the known optical dielectric constant of $2.2\varepsilon_0$. In this work we can relate only to the optical dielectric constant since we do not perform structural relaxation under applied bias, and therefore cannot capture the ionic contribution to the dielectric response. Within the limits of the electronic response around the interface, our permittivity profile agrees with earlier DFT studies [4],[17]. But the ionic contribution is not only responsible for the larger static dielectric constant of 3.9 of bulk oxide – it is behind the more significant enhancement of the interfacial permittivity in the oxide to $6\varepsilon_0$, as revealed in [17]. The present limitation in our work, with regards to the oxide stems from the lack of suitable parameterization for the repulsive interaction of Si and O in DFTB that is compatible with the electronic parameterization from [3], and must be addressed in the future.

IV. Conclusions

Atomic level simulations with DFTB Hamiltonian describe with sufficient accuracy both the bulk and interfacial dielectric properties of Si and SiO_2, although currently limited to the electronic response. Simulations confirm that the dramatic reduction of the Si channel that accompanies the downscaling of UTB-SOI devices leads to significant reduction of the permittivity of the channel. This qualitative trend is clear regardless of the Si-passivation used in the model. However, the simulations of oxidized Si film suggest more modest reduction (~18% at 0.8 nm Si thickness) as opposed to simulations with H-passivated channel (>30% at 0.8 nm). The influence of the interface effects is strong and it is difficult to capture quantitatively the trend by an analytical model that includes thickness dependent band-gap only.

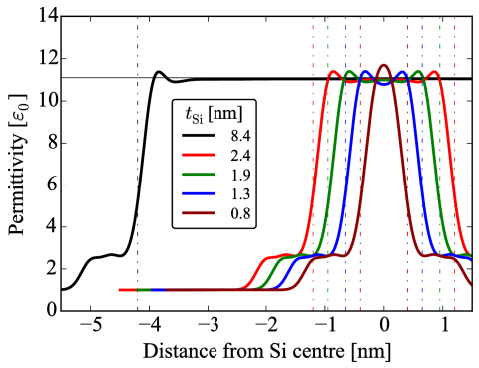

Fig. 7. Local permittivity profile $\varepsilon(y)$ for different Si film thicknesses. Note the weak variation of permittivity in the core of Si, as demonstrated also in [4]. In the limit of $t_{Si} \to \infty$ the core permittivity will be that of bulk. We take the convergent value of that to be our bulk value, which is $11.1\varepsilon_0$ (horizontal line), in good agreement with experimental value of $11.7\varepsilon_0$.

References

[1] P. Carrier, L. Lewis, and, M.W.C. Dharma-wardana, "Optical properties of structurally relaxed SiO/SiO_2 superlattices: The role of bonding at interfaces," *Phys. Rev. B*, Vol. 65, p.165339, 2002.

[2] Z. Lu and D. Grozea, "Crystalline Si/SiO2 quantum wells," *Appl. Phys. Lett.*, vol. 80, p. 255, 2002.

[3] S. Markov, B. Aradi, CY. Yam, H. Xie, T. Frauenheim, and GH. Chen, "Atomic level modeling of extremely thin silicon-on-insulator MOSFETs including the silicon dioxide: Electronic structure", *IEEE Trans. Elec. Dev.*, vol. 62, no. 3, pp. 696–704, 2015.

[4] F. Giustino, A. Pasquarello "Theory of atomic-scale dielectric permittivity at insulator interfaces", *Phys. Rev. B* **71** 144104, 2005.

[5] J. Nakamura, S. Ishihara, A. Natori, T. Shimizu, K. Natori, "Dielectric properties of H-terminated Si(111) ultrathin films," *J. Appl. Phys.* vol. 99, p. 054309, 2006.

[6] G. Zhang, M.B. Yu, C.H. Tung, G.Q. Lo, "Quantum size effects on dielectric constants and optical absorption of ultrathin silicon films," *IEEE Elec. Dev. Lett.*, vol. 29, p. 1302, 2008.

[7] H. Yoo, M. Fauchet, "Dielectric constant reduction in silicon nanostructures," *Phys. Rev. B* vol. 77, p. 115335, 2008.

[8] S. Markov, CY. Yam, B. Aradi, G. Penazzi, T. Frauenheim, and GH. Chen, "Towards atomic level simulation of electron devices including the semiconductor-oxide interface," in Proc. Simulation Semicond. Proc. and Dev., SISPAD, Yokohama, Japan, 2014.

[9] B. Aradi, B. Hourahine, Th. Frauenheim, "DFTB+, a sparse matrix-based implementation of the DFTB method," *J. Phys. Chem. A*, Vol. 111(26), p. 5678, 2007. Code available online: www.dftb-plus.info.

[10] Elstner, D. Porezag, G. Jungnickel, J. Elsner, M. Haugk, and Th. Frauenheim, *et al*, "Self-consistent-charge density-functional tight-binding method for simulations of complex materials properties," *Phys. Rev. B*, vol 58, pp. 7260–7268, Nov., 1998.

[11] T. Frauenheim, G. Seifert, M. Elstner, T. Niehaus, C. Köhler *et al*, "Atomistic simulations of complex materials: Ground-state and excited-state properties," *J. Phys.: Cond. Matt*, Vol. 14, p.3015, 2002.

[12] A. Pecchia, G. Penazzi, L. Salvucci, A. di Carlo, "Non-equilibrium Green's functions in density functional tight binding: method and applications," *New J. Phys*. vol. 10, p.065022, 2008.

[13] B. Meyer and D. Vanderbilt, "Ab initio study of $BaTiO_3$ and $PbTiO_3$ surfaces in external electric fields," *Phys. Rev. B* vol. 63, p.205426, 2001.

[14] S. Markov, P. V. Sushko, S. Roy, C. Fiegna, E. Sangiorgi, A. Shluger, and A. Asenov, "Si-SiO_2 interface band-gap transition – effects on MOS inversion layer," *Phys. Stat. Sol. (a)*, vol. 205, p1290, 2008.

[15] T. S. Moss, "Relation between the refractive index and band gap of semiconductors," *Phys. Stat. Sol. (b)*, vol. 131, p. 415, 1985.

[16] C. Delerue, M. Lanoo, and G. Allan, "Concept of dielectric constant for nanosized systems," *Phys. Rev. B*, vol. 68, p. 115411, 2003.

[17] N. Shi and R. Ramprasad, "Atomic-scale dielectric permittivity profiles in slabs and multilayers," *Phys. Rev. B*, vol. 74, p. 045318, 2006.